Biomass Conv. Bioref. (2018) 8:113–124
DOI 10.1007/s13399-016-0235-5

CrossMark

ORIGINAL ARTICLE

A study of black liquor and pyrolysis oil co-gasification in pilot scale

Yawer Jafri[1] · **Erik Furusjö**[1] · **Kawnish Kirtania**[1] · **Rikard Gebart**[1] · **Fredrik Granberg**[2]

Received: 13 October 2016 / Revised: 27 December 2016 / Accepted: 29 December 2016 / Published online: 14 January 2017

Abstract The effect of the blend ratio and reactor temperature on the gasification characteristics of pyrolysis oil (PO) and black liquor (BL) blends with up to 20 wt% PO was studied in a pilot-scale entrained-flow gasifier. In addition to unblended BL, three blends with PO/BL ratios of 10/90, 15/85, and 20/80 wt% were gasified at a constant load of 2.75 MW_{th}. The 15/85 PO/BL blend was used to investigate the effect of temperature in the range 1000–1100 °C. The decrease in fuel inorganic content with increasing PO fraction resulted in more dilute green liquor (GL), and a greater portion of the feedstock carbon ended up in syngas as CO. As a consequence, the cold gas efficiency increased by about 5%-units. Carbon conversion was in the range 98.8–99.5% and did not vary systematically with either fuel composition or temperature. Although the measured reactor temperatures increased slightly with increasing PO fraction, both unblended BL and the 15% PO blend exhibited largely similar behavior in response to temperature variations. The results from this study show that blending BL with the more energy-rich PO can increase the cold gas efficiency and improve the process carbon distribution without adversely affecting either carbon conversion or the general process performance.

Keywords Black liquor · Pyrolysis oil · Gasification · Pilot-scale · Co-gasification · Thermochemical conversion

1 Introduction

The development and large-scale deployment of cost-effective, liquid biofuels has been identified as a key to success in the de-fossilization of the transport sector. Biomass gasification is one of the pathways for biofuel production that has progressed towards commercialization in the past decade [1, 2]. Originally developed by Chemrec AB, the pressurized entrained-flow (EF) black liquor gasification (BLG) technology has now been demonstrated for 28,000 h at the 3 MW_{th} LTU Green Fuels pilot plant in Piteå, Sweden. Since its completion in 2005, the plant has been the site of several investigations into the gasification characteristics of black liquor (BL), which is a by-product of the pulping process [3–8]. The catalytic effect of BL alkali content ensures the production of a low-methane, tar- and soot-free syngas at residence times in the order of seconds and at temperatures around 1000–1050 °C [3]. Meanwhile, the pulping chemicals are recovered for reuse in a manner similar to that in a pulp mill with a recovery boiler.

The presence of the catalytic effect [9] and the existence of established supply chains in the pulp and paper industry [10] make BL uniquely suited to the production of syngas for subsequent biofuel production [11]. However, it is a hard-to-transport, energy-poor fuel whose availability is tied to pulp production at a given location. Blending BL with pyrolysis oil (PO), a similar yet more energy-rich fuel with none of the aforementioned disadvantages, offers a means of improving operational flexibility and increasing biofuel yield [12]. A techno-economic evaluation of PO/BL co-gasification showed that the use of a 25% PO blend could increase methanol production

Electronic supplementary material The online version of this article (doi:10.1007/s13399-016-0235-5) contains supplementary material, which is available to authorized users.

✉ Yawer Jafri
yawer.jafri@ltu.se

[1] Division of Energy Science, Luleå University of Technology, SE-971 87 Luleå, Sweden

[2] Green Fuels Operation, Luleå University of Technology, Industrigatan 1, 941 38 Piteå, Sweden

by 88% and energy efficiency by 4% compared to unblended BL [13].

The blending of BL with PO leads to a net decrease in fuel alkali content. It was seen in a study of coal-char gasification [14] that above an alkali/C atomic ratio ≈0.1, the catalytic activity of alkali reaches a saturation level. A similar effect may also be expected to exist for biomass. A few studies [15, 16] observed a linear increase in the gasification reactivity of biomass chars with increasing alkali content (alkali/C ratio <0.1). In another study [9], the opposite approach was adopted by reducing BL alkali content through incremental addition of PO. The char and droplet conversion rates of the resulting blends with up to 30% PO were found to be similar to those of unblended BL. Hence, the addition of PO did not affect the gasification reactivity of the BL/PO blends at all, thereby supporting the plateaued catalytic activity. However, none of these lab-scale (≤900 °C and atmospheric pressure) studies account for the high (flame) temperature as well as heating rate, and the resulting significant alkali release that is encountered in actual gasifiers. Moreover, syngas compositions and process energy efficiencies at different PO/BL blend ratios have only been estimated by simulation and, therefore, require validation, further study, and detailed experimental quantification in a more industrially representative scale.

The main aim of this study was to investigate, quantify, and assess the effect of the PO/BL blend ratio on syngas composition, sulfur distribution, carbon conversion, smelt composition, and cold gas efficiency in pilot scale under steady-state operation. A secondary aim was to study and compare the effect of reactor temperature on the gasification characteristics of a 15/85 PO/BL blend with those of unblended BL.

2 Material and methods

The BLG process consists of a pressurized, oxygen-blown EF gasifier with a refractory-lined reactor vessel, which converts sulfur- and alkali-rich BL, and blends thereof, into syngas and recoverable smelt. An overview of the major process components and media streams is shown in Fig. 1. A detailed schematic of all the media streams included in the mass and energy balances is provided in Appendix A1 in the Supplementary Information. Before it is sent to the synthesis plant, syngas is cooled to around 30 °C in two stages: initially in a direct quench and subsequently indirectly in a vertical gas cooler. In the process, it is stripped of particulates which are eventually recirculated back, together with condensed syngas tars, to a pool of liquid at the bottom of the gasifier that also contains the dissolved smelt in an aqueous solution named green liquor (GL). Further details can be found in an earlier parametric study [5] as well as in a recently published performance assessment of black liquor gasification [7].

The BL used in this study was taken from the neighboring Smurfit Kappa Kraftliner Piteå (SKKP) pulp mill, while the PO was produced at the Fortum bio-oil plant in Joensuu, Finland. In order to store and feed PO, a continuously stirred 2.2-m^3 day tank and two pumps were installed in the vicinity of the gasifier. The risk of lignin precipitation, which may occur due to the formation of pH gradients, was minimized by mounting a pressurized mixer before the gasifier, thereby ensuring thorough physical mixing of BL and PO. The co-gasification of the PO/BL blends did not require any modification of either the design of the burner nozzle or the operation of the existing gasifier feeding system.

2.1 Experimental conditions

During the experimental run, the gasifier was continuously operated on BL and three PO/BL blends at eight different settings. One of the BL settings was repeated in triplicate. Fuel feed data for all the unique operating points (OPs) is presented in Table 1. In total, more than 130 tons of Kraft BL and ~5 tons of PO were gasified over 5 days. In the present study, "standard operating conditions" denote a thermal load of 2.75 MW and a CH_4 content of 1.2 mol% in syngas, which was obtained by adjusting the oxygen flow to the reactor. This can be compared to a typical operating load of ~3.1 MW_{th} on BL. A slightly reduced thermal load was used to maximize operational stability and the potential for quantifying the effects of the investigated parameters.

The effect of the blending ratio was investigated by gasifying BL and blends with PO/BL ratios of 10/90, 15/85, and 20/80 on a mass basis at standard operating conditions. The effect of the reactor temperature was studied by operating the gasifier on a 15% PO blend at three different temperature settings denoted by syngas CH_4 fractions of 0.5%, 1.2%, and 2.1% and labeled "hot," "standard," and "cold," respectively. Although the day-tank capacity placed an upper limit on the duration of co-gasification experiments, all the OPs were in place for at least 6 h, which is three times the hydraulic residence time of GL. Due to the partial dissociation of organic acids found in PO, a temperature rise of 5–10 °C was observed in the mixer. However, the temperature of the fuel feed to the reactor was maintained between 140 and 145 °C by regulating the temperature of the BL to the mixer. A detailed breakdown of BL and PO compositions is presented in Table 2. In comparison with BL, PO contains significantly more carbon, marginally more oxygen, and virtually no ash. Meanwhile, a substantial fraction of the oxygen and carbon in BL is present as inorganic carbonates of sodium and potassium. Accordingly, PO has a considerably higher heating value than BL. Hence, at constant thermal load, the total fuel feed rate decreased with increasing PO fraction. The 10%, 15%, and 20% PO blends had PO/BL ratios of 17/83, 25/75, and 32/68, respectively, on an energy basis.

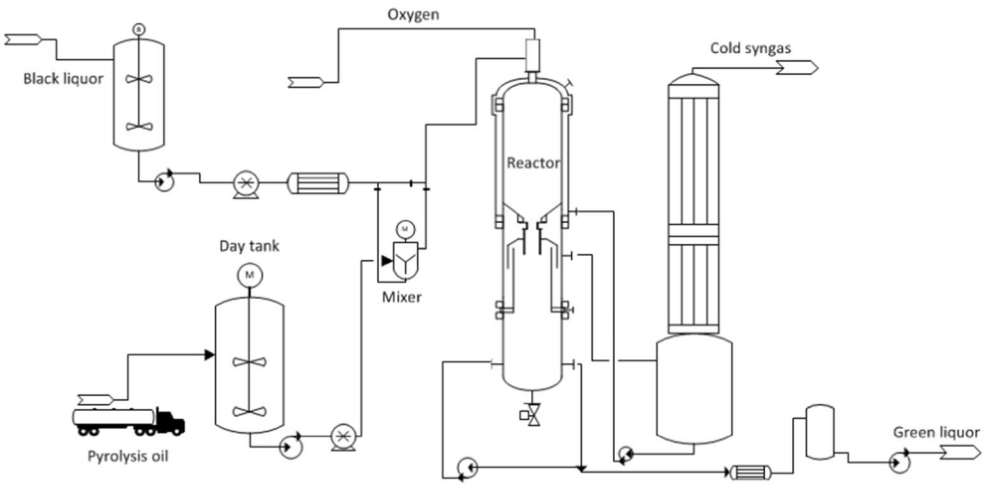

Fig. 1 The major process components and key media streams

A number of calibrations were performed to improve flow measurement accuracy, and they are discussed in more detail in section A1 of the Supplementary Information. Media samples from the study were analyzed at a number of laboratories, which are collated in Tables 2 and 3. Note that the general procedure used for the calculation of the energy balances was detailed recently [7]. The standard conditions used as the reference points for the calculation of BL standard enthalpy of combustion were defined as $T_{ref} = 25$ °C and $P_{ref} = 1$ bar, with K_2CO_3 (s), Na_2CO_3 (s), CO_2 (g), H_2O (l), and Na_2SO_4 (s) as the stoichiometric combustion products. The total titrable alkali (TTA) was calculated by summing the sulfide, carbonate, and bicarbonate concentrations.

2.2 Characteristic ratios

Similarly to coal, the difference in heating values between biomasses with low ash content has been correlated to differences in O/C and H/C ratios [17]. Although both of these ratios offer a useful means of fuel classification, they do not explicitly take into account the effect of variations in inorganic content on fuel properties such as heating value. Thus, for alkali-rich fuels like BL, a parameter such as alkali/C ratio, which decreases with increasing PO fraction, provides a more representative means of characterization. In the present work, the blends are classified in terms of their molar alkali-to-carbon ratio for quantitative comparisons.

The reactor temperature has been shown to be a nearly linear function of λ in entrained-flow gasification at steady-state conditions [18]. By definition, λ does not explicitly take into account variations in fuel oxygen content [19]. This can conceal the role played by the oxygen native to a fuel which, in most instances, is also available to the gasification reactions taking place in the reactor. In this study, the relative oxygen content (ROC) is used as a fuel-independent measure of the total oxygen available in the reactor. ROC, which has been used previously in studies on biomass gasification [20], is defined as follows [19]:

$$\mathrm{ROC} = \frac{O_{2\_additional} + O_{2\_fuel}}{O_{2\_stoich} + O_{2\_fuel}} \quad (1)$$

In Eq. 1, $O_{2\_additional}$ stands for gaseous oxygen added to the gasifier, O_{2_fuel} represents the fuel oxygen content, and O_{2_stoich} denotes the gaseous oxygen required for stoichiometric combustion. The λ values of all OPs are plotted as a function of ROC in Fig. 2. ROC and λ have a unique relationship

Table 1 The values of some key process variables for all the operating points (OPs)

	10% PO	15% PO Std.	20% PO	15% PO hot	15% PO cold
Black liquor (kg/h)	887	812	733	806	805
Pyrolysis oil (kg/h)	100	145	185	145	145
O_2/fuel (kg/kg)	0.310	0.313	0.326	0.331	0.307
Pressure (barg)	27.5	27.3	27.3	27.3	27.2
	BL-1 Std.	BL-2 Std.	BL-3 Std.	BL hot	BL cold
Black liquor (kg/h)	1103	1103	1102	1104	1100
Pyrolysis oil (kg/h)	0	0	0	0	0
O2/fuel (kg/kg)	0.296	0.289	0.289	0.299	0.278
Pressure (barg)	27.9	27.5	27.4	27.7	27.1

Table 2 Elemental analyses of black liquor (BL) and pyrolysis oil (PO) (on a wet basis)

	Unit	Average fraction	Lab	Measurement technique
Black liquor				
C	kg/kg BL	0.217[a]	SP[g]	Element analyzer
H	kg/kg BL	0.057[a]	SP[g]	Element analyzer
N	kg/kg BL	0.001[a]	SP[g]	Element analyzer
Cl	kg/kg BL	0.001[a]	SP[g]	Ion chromatograph
Na	kg/kg BL	0.139[b]	ALS[h]	ICP-AES[c]
K	kg/kg BL	0.026[b]	ALS[h]	ICP-AES[c]
S	kg/kg BL	0.045[b]	ALS[h]	ICP-AES[c]
O	kg/kg BL	0.514	–	By difference
Dry solids	kg DS/kg BL	0.732	LTU GF[i]	Drying and weighing
HHV BL[a]	MJ/kg DS	11.75	SP[g]	Bomb calorimetry
LHV BL[a]	MJ/kg BL	7.91	–	From HHV BL
Pyrolysis oil				
C	kg/kg PO	0.376	VTT[j]	CHN analyzer[d]
H	kg/kg PO	0.078	VTT[j]	CHN analyzer[d]
N	kg/kg PO	0.001%	VTT[j]	CHN analyzer[d]
O	kg/kg PO	0.545%		By difference
Dry solids	kg DS/kg PO	0.701	VTT[j]	Karl Fischer titration[e]
TAN	mg KOH/g	64.4	VTT[j]	Potentiometric titration[f]
HHV PO	MJ/kg DS	16.84	LTU EN[k]	Bomb calorimetry
LHV PO	MJ/kg PO	15.12	–	From HHV using composition data

[a] Calculated from two samples taken at the beginning and the end of the experimental run

[b] Calculated from ten samples spread over the experimental run

[c] SS EN ISO 11885 (modified)

[d] ASTM D 5291

[e] ASTM E 203

[f] ASTM D 664

[g] SP Research Institute of Sweden (Borås)

[h] ALS Scandinavia, Luleå

[i] LTU Green Fuels Plant (internal)

[j] VTT Technical Research Centre of Finland Ltd.

[k] LTU ENE Lab

for each distinct fuel composition, which is determined by both the oxygen content of a fuel and the amount of added gaseous oxygen. This is exemplified by the positions of the lines representing pure BL and the 15% PO blend relative to each other. However, for a given blend ratio, each point along the λ-ROC line represents variations in the amount of added gaseous oxygen alone, which in turn are caused by changes in desired operating temperatures. A comparison of the 10% PO OP with one of the pure BL OPs shows that fuels with different compositions can give rather similar λ values even when their gasification is likely to produce syngas with significantly different compositions. However, the differences between fuels are more clearly distinguishable in the ROC values, which capture variations in fuel oxygen content explicitly. Hence, compared with the λ value, ROC is believed to be better suited for directly comparing and assessing the effect of fuel composition on certain gasification performance parameters of varied biomass-based feedstocks.

Although Fig. 2 is based on a constant PO and BL solids composition (Table 2), it does incorporate the effect of variations in BL solids fraction, which are chiefly responsible for any deviations from the straight line. The solids fraction in BL from the SKKP mill has been shown to vary cyclically [7], and it went down by nearly 2% over the course of the present experimental run. On Fig. 2, the standard OP lies much closer to the cold OP than to the hot OP for the 15% PO blend. Since additional oxygen requirement is determined by controlling syngas methane content, the amount needed to reach the set value of 1.2% was less than expected. One potential cause may be an uncontrolled variation in BL solids composition, which led to a small decrease in BL carbon content, and thus the oxygen demand.

Table 3 Analytical methods used for the determination of medium concentration

Media	Component	Lab	Measurement method	Standard
Green liquor	Na, K, S	ALS[d]	ICP-AES	SS EN ISO 11885 (modified)
	Filtrate TIC[a]	MoRe[e]	TOC analyzer[h]	ISO 8245
	Filtrate TOC[b]			ISO 8245
	Suspended solids "sludge" content		Filtration	T 692 om -93
	CO_3^{2-}, HCO_3^-		Acid titration	SCAN-N 32
	HS^-			SCAN-N 31
	$HCOO^-$[c]	Innventia[f]	IC-CD[i]	Information Not Available
Condensate	Na, K, S	ALS[d]	ICP-AES	SS EN ISO 11885 (modified)
	TIC	MoRe[e]	TOC analyzer[h]	ISO 8245
	TOC			ISO 8245
Syngas	All components	SP ETC[g]	Gas chromatography[j]	Information Not Available

[a] Total inorganic carbon
[b] Total organic carbon
[c] Formate ion
[d] ALS Scandinavia, Luleå
[e] MoRe Research, Örnsköldsvik
[f] Innventia AB, Stockholm
[g] SP Energy Technology Center, Piteå
[h] Shimadzu, Model TOC-5050
[i] Ion chromatography with conductivity detection
[j] Varian CP-3800

In view of the likely applications, BLG energy efficiency was quantified using three different parameters on a LHV basis. CGE_{power} takes into account the heating value of all syngas components. CGE_{fuel} only considers CO and H_2, the two most important components for chemical synthesis, while $CGE_{fuel\ +\ S\text{-}free}$ is calculated on a sulfur-free basis to capture the importance of sulfur recovery to the pulp mill [7].

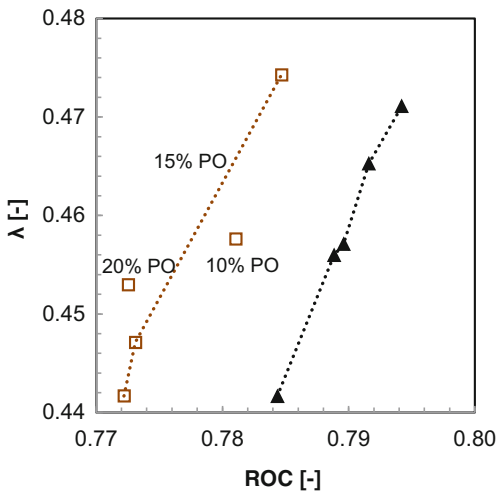

Fig. 2 λ as a function of ROC for BL (*triangles*) and the PO/BL blends (*squares*). Increasing values along the λ-ROC lines denote increasing temperature

Similarly, the carbon conversion efficiency used in the present study was recently defined as follows [7]:

$$\eta_{carbon} = \left(1 - \frac{m_{C,\ TOC}}{m_{C,fuel}}\right) * 100 \quad (2)$$

In Eq. 2, $m_{C,\ fuel}$ is the mass flow rate of fuel carbon, η_{carbon} is the carbon conversion efficiency, and $m_{C,\ TOC}$ is the mass flow rate of the dissolved organic carbon in GL (GL TOC). For pure BL OPs, $m_{C,\ fuel}$ was equal to the mass flow rate of carbon in BL ($m_{C,\ BL}$) while for the blends, it was determined by adding together $m_{C,\ BL}$ and the carbon in PO ($m_{C,\ PO}$). The $m_{C,\ BL}$ was calculated by multiplying the averaged weight fraction of carbon in BL solids obtained from the ultimate analysis of two separate samples by the solids fraction and the mass flow rate of BL for a given OP. Meanwhile, the $m_{C,\ PO}$ was obtained by multiplying the weight fraction of carbon in wet PO solids by the mass flow rate of PO. Similarly, $m_{C,\ TOC}$ for each OP was calculated by multiplying the GL mass flow rate by the mass fraction of the dissolved organic carbon (TOC).

Note that the definition in Eq. 2 does not account for potential accumulation of char in the system. However, it is worth recalling that the quenching and cooling of syngas take place in a wet environment. The design of the cooling system ensures that both condensed tars from syngas and unconverted carbon fragments from the reactor end up and leave the

gasifier in the liquid GL. Hence, char build-up is considered unlikely to occur under steady-state operation, as supported by the experience gained from continuous plant operation over long periods [1].

3 Results and discussion

Overall, mass balance closures ranged from 94% to 100% and averaged 97% for both BL and the blends. The deviations appeared to be independent of fuel composition. In terms of individual elements, the deviations in carbon balance closures did not exceed 4% for any of the OPs. In contrast, sulfur balance closures averaged 104% and returned a standard deviation of 7.4%, with a maximum deviation of 19%. On the other hand, energy balance closures did not deviate by more than 5%, which was in agreement with recent observations [7]. See Appendices A1 and B1 in the Supplementary Information for an extended discussion and a detailed breakdown of the overall mass and energy balances by operation point.

3.1 Syngas composition

While the CO_2 content in syngas decreased with increasing PO fraction, the CO and H_2 contents increased almost linearly, as shown on Fig. 3a. Since the increase was less pronounced for H_2, the H_2/CO ratio decreased from 1.36 for BL to 1.23 for the 20% PO blend. Seeing as the fuel inorganic content decreased with increasing PO fraction, the increases in H_2 and CO yields can be attributed to the resultant reduction in reactor thermal ballast, which meant that fewer oxidation reactions were required to reach the gasification temperature. Accordingly, the amount of carbon bound to sodium and potassium in smelt also decreased with increasing PO fraction. The effect was so pronounced that, in spite of 5%-points lower fuel carbon throughput compared with BL, the 20% PO blend actually resulted in a higher combined yield of CO and CO_2 on a mass basis. Overall, the use of a 20% PO blend instead of pure BL yielded a 17% reduction in the additional oxygen demand per mole of H_2 + CO produced.

Figure 4a shows that the standard temperature setting, which is denoted by a syngas CH_4 fraction of 1.2 mol%, yielded the highest CO and H_2 flow rates for both BL and the 15% PO blend. The increase in reactor temperature from the cold to the standard setting led to a 7% increase in H_2 flow rate. However, a further increase in temperature promoted the production of CO_2 at the expense of CO, while the H_2 flow rate also exhibited a marginal fall.

The ROC value of a given fuel can be calculated easily provided composition data is available. Hence, in addition to use as a means of differentiation between fuels, under certain circumstances it can also be used as a tool for

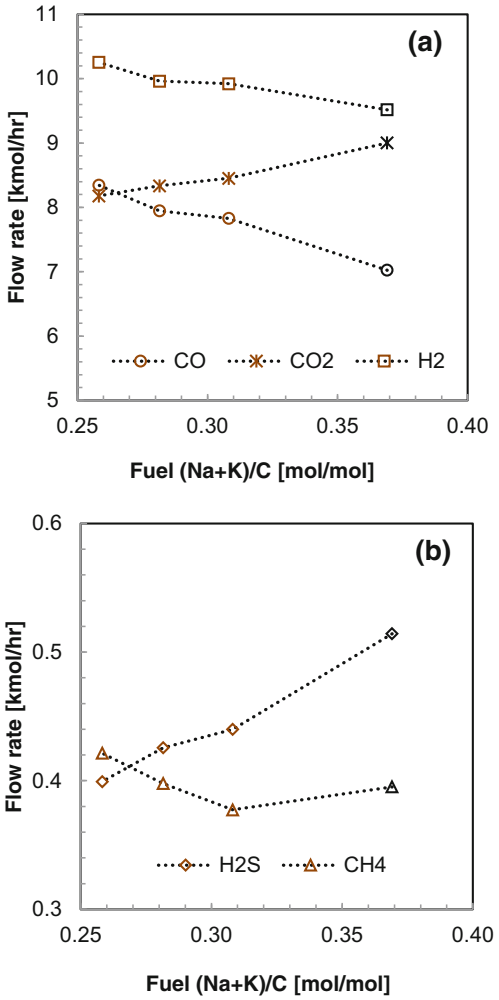

Fig. 3 The change in the amounts of **a** CO, CO_2, and H_2 as well as **b** H_2S and CH_4 with the blend ratio (0–20%) at approximately constant syngas methane content

predicting yields of major syngas species as a function of fuel oxygen content. On Fig. 4a, the flow rates of H_2, CO, and CO_2 for the six points representing four different fuel compositions show a partial correlation with ROC to varying degrees. The yields of all three components are determined by the water-gas shift reaction controlled by thermodynamic equilibrium. Moreover, as was alluded to in Section 2.2, due to the effect of changes in, e.g., the alkali/C ratio, parameters such as heating value and by extension gasification temperature and additional oxygen vary non-linearly with the O/C and the H/C ratios. This is partly responsible for the inability to qualitatively identify variations in fuel composition from changes in ROC alone. At the same time, the absence of a correlation with the rate-controlled CH_4, and to a lesser extent the only partially equilibrium-controlled H_2S, can be seen clearly in Fig. 4b. In the case of CH_4, the changes in yield are solely a function of temperature, which is regulated by the amount of added oxygen, and thus described adequately by λ.

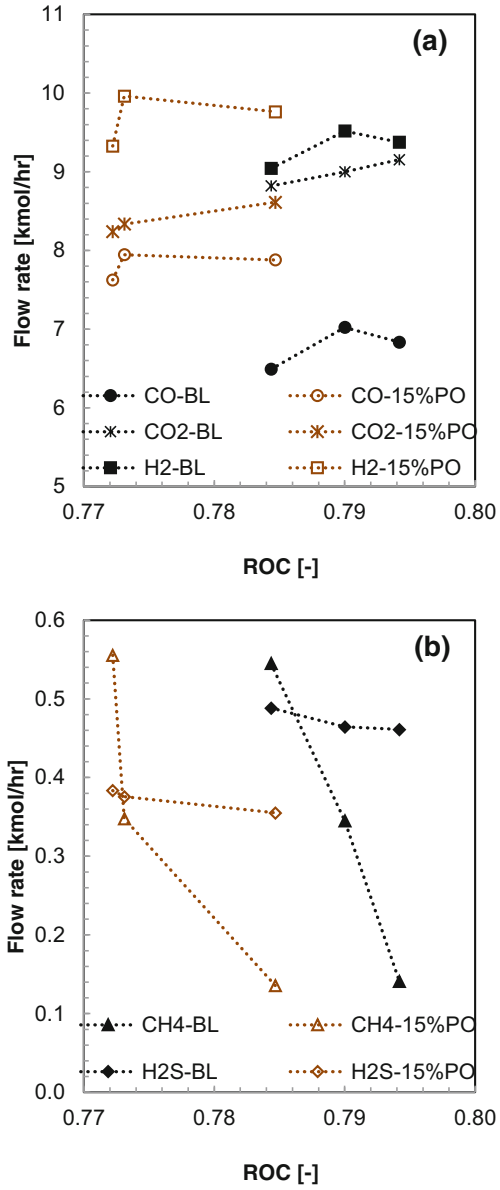

Fig. 4 The changes in **a** syngas CO, CO_2, and H_2 as well as **b** syngas H_2S and CH_4 contents with temperature for BL and a 15% PO blend. Increasing ROC values denote increasing temperature

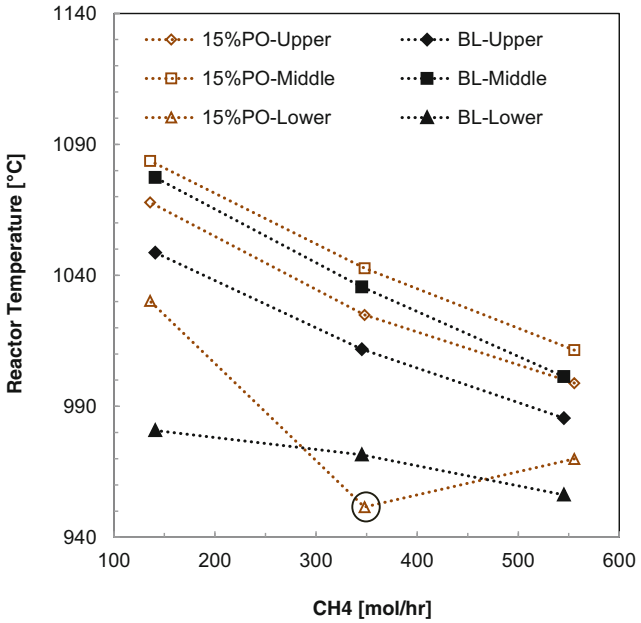

Fig. 5 The correlation between reactor temperature and CH_4 for both pure BL and the 15% PO blend. The upper, middle, and lower arrays represent temperature measurements along the length of the reactor

3.2 Reactor temperature

The temperatures recorded by thermocouples (TCs) at three different positions along the reactor length are plotted in Fig. 5 for both the PO/BL blends and pure BL as a function of their CH_4 content at the cold, standard, and hot temperature settings. In comparison with BL, the 15% PO blend yielded slightly higher temperatures at all three positions for the same CH_4 content. The results in Fig. 5 also confirm that the good correlation between the measured temperatures and syngas CH_4 for BL [8] holds true for the PO/BL blends as well. For the 15% PO blend, the correlation coefficients between the upper, middle, and lower temperatures and CH_4 were −0.99, −1.00, and −0.74. The thermocouple in the lower part of the reactor returned erratic readings both during and after the run that is circled on Fig. 5. The measured value is likely an underestimate and the erratic behavior may have been caused by a temporary build-up of smelt. In general, the correlations are particularly good for the upper and middle arrays which are located closer to the flame than the lone bottom TC, which is more likely to provide readings representative of the syngas temperature at the reactor exit. Note that the present results are in agreement with observations that were made during the gasification of sulfite thick liquor in an earlier study. [8]

The temperature readings from the TCs mounted in the reactor wall are susceptible to conductive interference from the wall and radiation from the very hot flame in the upper part of the reactor. However, experience has shown that the recorded readings can consistently reflect and mirror changes in operating conditions over a single experimental run. The temperature rises recorded in the present study are believed to be inconsequential in terms of their impact on the life of the refractory lining.

Syngas from the blends was very clean as, irrespective of fuel composition, C_6H_6 was the only higher hydrocarbon present in amounts greater than 20 ppm. Figure 6 shows that the flow rate of C_6H_6 increases with increasing CH_4 for both BL and the 15% PO blend. Interestingly, the blend yielded noticeably less C_6H_6 than BL at nearly the same CH_4 flow rate and the difference grew larger with decreasing temperature. The phenomenon is currently under investigation.

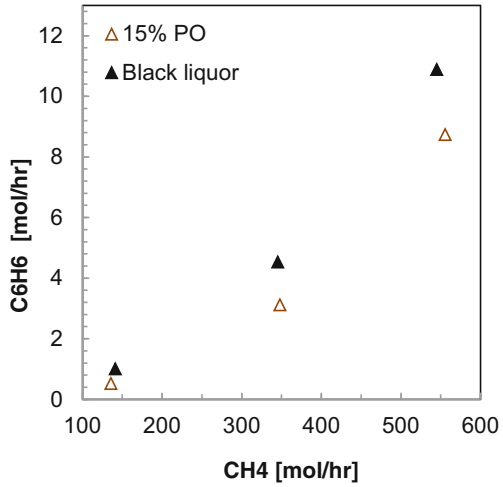

Fig. 6 The flow rate of C_6H_6 as a function of CH_4 (and thus temperature) for both BL and the 15% PO blend. Decreasing CH_4 and C_6H_6 contents denote increasing temperature

3.3 Sulfur release

The fraction of feedstock sulfur released as H_2S, which is also referred to as the sulfur split, varied between 31% and 35% for the PO/BL blends and 28–31% for BL. Figure 3b shows that the decrease in fuel sulfur content with increasing PO fraction resulted in a corresponding decrease in the amount of sulfur release as H_2S. As shown on Fig. 4b, the H_2S flow rate decreased by 6–7% between the hot and the cold temperature settings for both BL and the 15% PO blend. The extent of the sulfur released in gaseous form has been shown to reach a maximum at ~500–600 °C [21], and higher temperatures are thought to favor sulfur recapture [22]. The sulfur that is either recaptured by volatilized sodium or retained in smelt reacts with steam and CO_2 according to the reaction in Eq. 3.

$$Na_2S\,(l) + H_2O(g) + CO_2(g) = Na_2CO_3(l) + H_2S\,(g) \rightarrow \Delta H_r = -169.8\ \mathrm{kJ}/\mathrm{mol} \quad (3)$$

A thermodynamic equilibrium study of BLG found around two thirds of the feedstock sulfur in the gas phase as H_2S at temperatures above 800 °C and pressures above 20 bar [6]. However, the sulfur split for both the blends and BL shows that this was clearly not the case in the present study. Consequently, the reaction in Eq. 3 is only in partial thermodynamic equilibrium, and the final division of fuel sulfur between smelt and syngas at the exit of the reactor is also subject to kinetic limitations.

According to Le Chatelier's Principle, an increase in reactor temperature would be expected to lead to an increase in Na_2S formation at the expense of H_2S, as the reaction in Eq. 3 shifts to the left. A partial shift did occur, as the fraction of gas-phase sulfur decreased with temperature by up to 4%-points for both BL and the 15% PO blend. On the other hand, the split was found to increase with PO fraction, by up to 6%-points for the 20% PO blend. In this case, the partial equilibrium is affected not only by the temperature, which increases only slightly with PO fraction, but also by the significant variations in the concentrations of the gaseous components.

Similar to previous studies [4, 7], a trivial amount of sulfur was also released in the form of COS at all OPs. The release was in the range 83–96 ppm, and it was not possible to identify any correlation with fuel composition due to the hydrolysis of COS in the quench tube [4]. The molar fraction of N_2 in syngas did not exceed 1.6% for any of the OPs. As the temperature of the gasification products falls after entering the quench tube, the water-gas shift reaction produces more CO_2 and H_2. The extent of this shift, which is influenced by the orientation and flow rate of the cooling sprays [4], could not be quantified, but the spray flow rates were set at 600 kg/h to ensure constant cooling rates.

3.4 GL composition

Table 4 shows that aside from HCO_3^-, which is dependent upon the magnitude of CO_2 absorption, the flow rate of the other elements and ions decreased in proportion, albeit not wholly, with the fuel inorganic fraction. Consequently, with the exception of the slightly anomalistic 15% PO OP, the GL became more dilute with an increasing PO fraction. In principle, the elemental concentrations in GL are a product of fuel inorganic content and the amount of water added to the GL dissolver through the three water streams shown on Fig. A.1 in the Supplementary Information. Although these streams provide a means of regulating GL concentration, due to the design and present setup of the cooling system, the range of possible concentrations is constrained by limits on minimum flows. Hence, in the interest of maximizing operational stability, the water flows into the GL dissolver were not reduced in proportion to the expected reduction in smelt flow. In theory, the system can be optimized to better regulate inflows and increase the TTA by rebuilding the lower part of the gasifier. It has previously been shown that some of the syngas CO_2 is absorbed in the GL [4], which results in the destruction of OH^- and the formation of HCO_3^- ions. The concentrations of these ions, which were present in all GL samples, did not appear to vary systematically with fuel composition.

In Kraft pulping, any sulfur present in a form other than Na_2S or K_2S does not play an active role in the cooking process, which means that sulfide reduction efficiency needs to be maximized. Sulfur reduction efficiency values of 100% within measurement uncertainty limits had previously been reported in an earlier study on the gasification of spent sulfite liquor [8]. Interestingly and somewhat unexpectedly, as seen in Table 4, the HS^- concentrations found in the GL were consistently lower than total S concentrations for both BL and the blends. At the same time, the correlation coefficient between the HS^-

Table 4 The concentrations of the most important ions and elements in green liquor from the three pyrolysis oil/blends

	BL only[b]	10% PO	15% PO	20% PO
S (mol/L)[a]	0.51	0.36	0.39	0.29
Na (mol/L)[a]	3.20	2.14	2.36	1.84
K (mol/L)[a]	0.34	0.24	0.26	0.20
HCO_3^- (mol/L)	0.21	0.18	0.18	0.21
HS^- (mol/L)	0.42	0.30	0.30	0.27
CO_3^{2-} (mol/L)	1.27	0.95	0.92	0.82
$HCOO^-$ (mol/L)	0.03	0.02	0.02	0.03
Total titrable alkali (mol/L)	3.54	2.38	2.62	2.04
$(S + 2*CO_3^{2-} + HCO_3^-)/(Na + K)$ (mol/mol)	95%	103%	92%	104%
Sulfidity—$S/(Na + K)_2$ (mol/mol)	28.9%	29.9%	29.8%	28.5%

[a] S, Na, and K concentrations have a measurement uncertainty of 10%

[b] The concentrations are averages of measurements from BL OPs at the same thermal load as the PO/BL blends

and the total S concentrations was 0.90, which supported the relative accuracy of the measurements. The methods used for the determination of HS^- and total S concentrations in GL have specified relative measurement uncertainties of 15% and 10%, which is of the same order of magnitude as the differences between the values (10–30% relative to HS^-). Moreover, GL from the BLG pilot plant is extremely sensitive to oxidation during sample preparation, which makes the quantification of reduced sulfur forms, such as sulfide ions, very difficult. Consequently, a complete characterization of the GL sulfur species could not be carried out. Given the high reduction efficiencies seen previously, the differences between total S and HS^- concentrations may be due to systematic analysis-related errors. Nonetheless, in light of the above results and given the significance of sulfur recovery, the possibility of the presence of non-reduced forms of sulfur in GL needs to be considered in future work.

The changes in the total organic carbon, total inorganic carbon, and sludge content with increasing PO fraction are shown in Fig. 7. GL sludge fractions and TOC concentrations in the GL filtrate from both the blends and BL were comparable and did not vary systematically. In contrast, as expected, the TIC content decreased linearly since it is directly related to fuel inorganic content. Carbon found in formate ions constituted 23–41% of the TOC in the GL filtrate from the PO/BL blends and 24–49% from BL. The rest of the GL TOC is believed to be mainly tars condensed during quenching and gas cooling as discussed in a recent publication [7]. However, in the absence of a method for detailed TOC characterization, it is not possible to go much beyond reasoned speculation. In the aforementioned study, the carbon present as formate had made up 10–28% of GL TOC and measured formate concentrations had correlated reasonably well with the partial pressure of the CO in syngas [7]. However, such a correlation was not found here for reasons that are not presently clear.

Figure 8 shows that, irrespective of fuel composition, neither GL TIC nor GL sludge showed a meaningful change with temperature. While GL TOC did vary for both BL and the 15% PO blend, the changes did not appear to be systematic. In both Figs. 7 and 8, the error bars on the TOC concentrations represent an estimated measurement uncertainty of 15%. It can be seen that although the uncertainties overlap partially, the range of the variations exceeds measurement uncertainty, which was also found to be the case in an earlier study [7]. Coupled to the fact that TOC variations did not appear to be a function of the most probable process parameters such as fuel composition, temperature, or load, this points to the presence of currently unknown, non-controllable factors which influence GL TOC.

3.5 Carbon conversion efficiency

The gasification of the PO/BL blends yielded carbon conversion efficiencies of 98.8–99.5%. These values increase to 99.0–

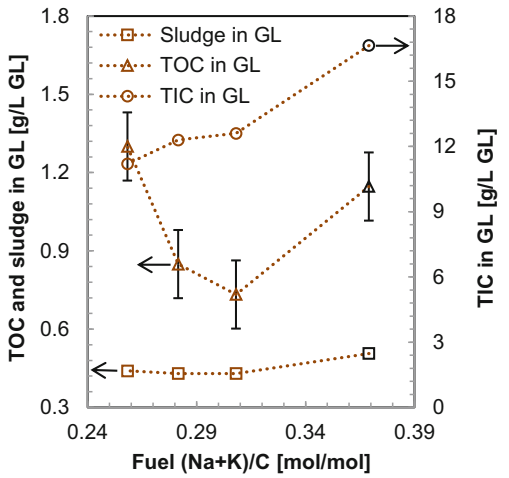

Fig. 7 The effect of the blend ratio (0–20%) on sludge (*left vertical axis*), TOC (*left vertical axis*), and TIC (*right vertical axis*) concentrations in GL

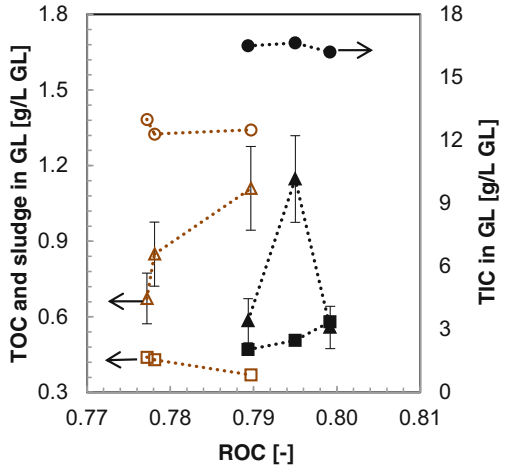

Fig. 8 The variation in suspended solids (sludge) (*square*: *left vertical axis*), TOC (*triangle*: *left vertical axis*), and TIC (*circle*: *right vertical axis*) contents in green liquor with temperature for BL (*solid*) and the 15% PO blend (*hollow*). Increasing ROC values denote increasing temperature

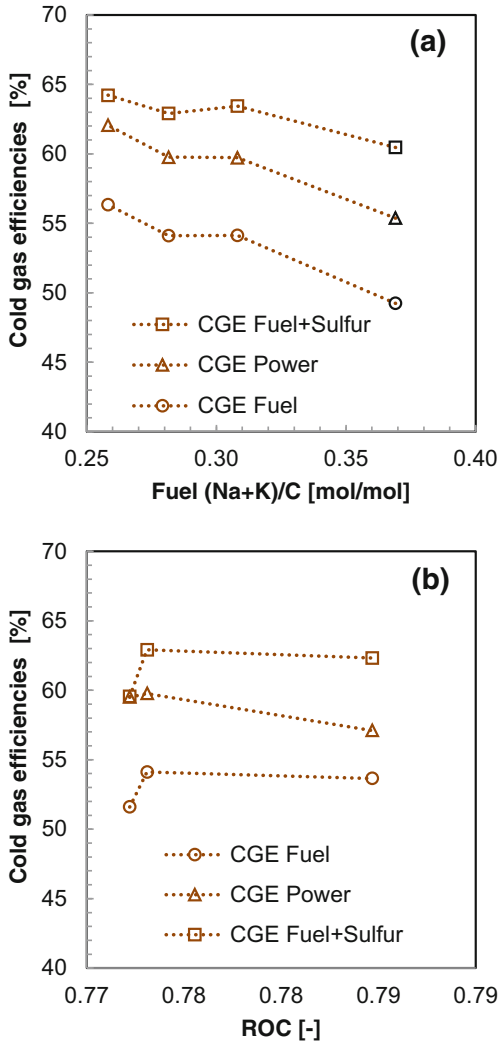

Fig. 9 CGE_{power}, CGE_{fuel}, and $CGE_{fuel\ +\ S\text{-}free}$ on LHV basis for **a** the different fuel blends at standard temperature and **b** the 15% PO blend at varying temperatures. Increasing ROC values denote increasing temperature

99.7% if the carbon present as formate in GL is considered "converted" for the purpose, given its hypothesized origin in syngas CO. The completeness of conversion was also supported by the absence of any detectable unconverted char in GL. Char gasification is the rate-limiting step controlling carbon conversion, and it is greatly facilitated by the intrinsically high reactivity of alkali-rich BL char [9]. A plot of the carbon conversion efficiencies for all the OPs as a function of their ROC values (not shown) found there to be no correlation between the two variables. It may thus be concluded that the changes in η_{carbon} were independent of changes in blend ratio, fuel composition, and temperature. As a corollary, the decrease in alkali loading with increasing PO fraction did not have a discernible effect on carbon conversion in the range studied.

3.6 Cold gas efficiency

In energetic terms, the value of increasing the PO fraction at a constant thermal load can be clearly seen from Fig. 9a. As discussed in Section 3.1, the CO and H_2 contents in syngas increased markedly with the increasing PO fraction at the expense of CO_2. As a result, both CGE_{power} and CGE_{fuel} also increased. In comparison with BL, the 20% PO blend yielded a 7%-point higher CGE_{fuel}, a 7%-point higher CGE_{power}, and a 5%-point higher $CGE_{fuel\ +\ S\text{-}free}$. $CGE_{fuel\ +\ S\text{-}free}$ is the ratio of syngas LHV_{fuel}, which is presented in Table B.2 of the Supplementary Information, and fuel $LHV_{S\text{-}free}$, which is influenced by the fuel S fraction. The decrease in syngas H_2S content with the increasing PO fraction meant that while it accounted for, on average, approximately 5% of LHV_{power} in the syngas from the BL, the same figure dropped to only 3.4% in the syngas from the 20% PO blend.

Figure 9b shows that due to the presence of CO and H_2 yield maxima, the potential for fuel production peaked at the standard temperature setting. Syngas contained significantly less CO and H_2 at the lower temperature setting, while at the higher temperature setting, some of the CO was oxidized to CO_2, thereby resulting in a slightly lower CGE_{fuel}. Meanwhile, changes in CGE_{power} are closely linked to the CH_4 content of syngas for a given fuel composition. At the cold temperature setting, CH_4 made up approximately 9% of syngas LHV. Due to the conversion of some of this CH_4 into CO and CO_2, the share dropped to 5–6% at the standard temperature setting. Consequently, CGE_{power} at the standard temperature might be expected to be slightly lower, but as can be seen from Fig. 9b, the values of CGE_{power} at the high and standard settings are very similar, which is very likely due to experimental error. At the hot temperature setting, much of this CH_4 was converted to CO_2, thereby leading to a decrease

in the syngas heating value. It is likely that the standard temperature setting represents a close-to-optimal point for biofuel production within the operating envelope of the gasifier.

4 Concluding remarks

The results of this study demonstrate that a pilot plant designed for the gasification of BL needs only minor modifications, such as the addition of a PO/BL mixer, in order to successfully gasify PO/BL blends. In general, the blending of BL with PO had a notably positive impact on the performance of the gasification process. Importantly, carbon conversion did not vary systematically with fuel composition, which shows quite clearly that the addition of up to 20% PO on a mass basis does not degrade the catalytic activity of BL Na. There were no signs of an increase in either soot or tar formation. The blends yielded cold gas efficiencies that were markedly greater in comparison to those of BL at the same thermal load.

The composition of syngas from unblended BL and the 15% PO blend exhibited largely similar behavior in response to changes in temperature; in both cases, the standard temperature setting appeared to represent the optimum for biofuel production. In comparison with unblended BL, the oxygen consumption of PO/BL blends was higher per kilogram of feed, but lower per MW of syngas H_2 + CO. It is believed that ROC can be useful as a tool for predicting trends in yields of major syngas species from ash-free biomass feedstocks for varying feedstock composition and gasification temperature.

The fate of sulfur is of significant consequence to the recovery of pulping chemicals and the integration of BLG with a pulp mill. The fraction of sulfur that ends up in the syngas was somewhat higher for the PO/BL blends than for BL. Due to analytical difficulties, the sulfur reduction efficiency was uncertain. Based on the results of this study, the gasification of blends with even higher PO fractions appears to be practically feasible. The mixing characteristics of the PO/BL blends are currently the subject of active research. Future work in this area is needed on (i) method development for better characterization of GL TOC, (ii) quantification of the effect of long-term variations in fuel composition on process performance, and (iii) the study of the sulfur chemistry in GL and the syngas cooling system.

Acknowledgments The operating staff at the LTU Green Fuels pilot plant is acknowledged for their skilled work during the experiments.

Compliance with ethical standards

Source of funding This work was supported by the Swedish Energy Agency and the industry consortium in the LTU Biosyngas Program. The funders were not involved in study design; in the collection, analysis, and interpretation of data; in the writing of the manuscript; and in the decision to submit the article for publication.

References

1. Landälv I, Gebart R, Marke B, Granberg F, Furusjö E, Löwnertz P et al (2014) Two years experience of the BioDME Project—a complete wood to wheel concept. Environ Prog Sustain Energy 33:744–750
2. Haro P, Johnsson F, Thunman H (2016) Improved syngas processing for enhanced Bio-SNG production: a techno-economic assessment. Energy 101:380–389. doi:10.1016/j.energy.2016.02.037
3. Öhrman O, Häggström C, Wiinikka H, Hedlund J, Gebart R (2012) Analysis of trace components in synthesis gas generated by black liquor gasification. Fuel 102:173–179. doi:10.1016/j.fuel.2012.05.052
4. Wiinikka H, Carlsson P, Marklund M, Grönberg C, Pettersson E, Lidman M et al (2012) Experimental investigation of an industrial scale black liquor gasifier. Part 2: influence of quench operation on product gas composition. Fuel 93:117–129. doi:10.1016/j.fuel.2011.06.066
5. Carlsson P, Wiinikka H, Marklund M, Grönberg C, Pettersson E, Lidman M et al (2010) Experimental investigation of an industrial scale black liquor gasifier. 1. The effect of reactor operation parameters on product gas composition. Fuel 89:4025–4034. doi:10.1016/j.fuel.2010.05.003
6. Carlsson P, Marklund M, Furusjö E, Wiinikka H, Gebart R (2010) Experiments and mathematical models of black liquor gasification—influence of minor gas components on temperature, gas composition, and fixed carbon conversion. TAPPI J 9:15–24
7. Jafri Y, Furusjö E, Kirtania K, Gebart R (2015) Performance of an entrained-flow black liquor gasifier. Energy Fuel. doi:10.1021/acs.energyfuels.6b00349
8. Furusjö E, Stare R, Landälv I, Löwnertz P (2014) Pilot scale gasification of spent cooking liquor from sodium sulfite based delignification. Energy Fuel 28:7517–7526. doi:10.1021/ef501753h
9. Bach-Oller A, Furusjö E, Umeki K (2014) Fuel conversion characteristics of black liquor and pyrolysis oil mixtures: efficient gasification with inherent catalyst. Biomass Bioenergy 79:155–165. doi:10.1016/j.biombioe.2015.04.008
10. Consonni S, Katofsky RE, Larson ED (2009) A gasification-based biorefinery for the pulp and paper industry. Chem Eng Res Des 87:1293–1317. doi:10.1016/j.cherd.2009.07.017
11. Edwards R, Hass H, Larivé J-F, Lonza L, Mass H, Rickeard D. (2014) Well-to-wheel analysis of future automotive fuels and powertrains in the European context, well-to-wheels Appendix 2 - Version 4.a, reference list. doi:10.2790/95533.
12. Andersson J, Furusjö E, Wetterlund E, Lundgren J, Landälv I (2016) Co-gasification of black liquor and pyrolysis oil: evaluation of blend ratios and methanol production capacities. Energy Convers Manag 110:240–248. doi:10.1016/j.enconman.2015.12.027
13. Andersson J, Lundgren J, Furusjö E, Landälv I (2015) Co-gasification of pyrolysis oil and black liquor for methanol production. Fuel 158:451–459. doi:10.1016/j.fuel.2015.05.044

14. Wood BJ, Sancier KM (1984) The mechanism of the catalytic gasification of coal char—a critical-review. Catal Rev Eng 26:233–279
15. Struis RPWJ, von Scala C, Stucki S, Prins R et al (2002) Gasification reactivity of charcoal with CO_2. Part II: metal catalysis as a function of conversion. Chem Eng Sci 57:3593–3602. doi:10.1016/S0009-2509(02)00255-5
16. Perander M, DeMartini N, Brink A, Kramb J, Karlström O, Hemming J et al (2015) Catalytic effect of Ca and K on CO2 gasification of spruce wood char. Fuel 150:464–472. doi:10.1016/j.fuel.2015.02.062
17. Prins MJ, Ptasinski KJ, Janssen FJJG (2007) From coal to biomass gasification: comparison of thermodynamic efficiency. Energy 32:1248–1259. doi:10.1016/j.energy.2006.07.017
18. Weiland F, Wiinikka H, Hedman H, Wennebro J, Pettersson E, Gebart R (2015) Influence of process parameters on the performance of an oxygen blown entrained flow biomass gasifier. Fuel 153:510–519. doi:10.1016/j.fuel.2015.03.041
19. Stemmler M, Müller M (2010) Theoretical evaluation of feedstock gasification using H2/C ratio and ROC as main input variables. Ind Eng Chem Res 49:9230–9237. doi:10.1021/ie100726b
20. Weiland F, Nordwaeger M, Olofsson I, Wiinikka H, Nordin A (2014) Entrained flow gasification of torrefied wood residues. Fuel Process Technol 125:51–58. doi:10.1016/j.fuproc.2014.03.026
21. Whitty K, Kullberg M, Sorvari V, Backman R, Hupa M (2008) Influence of pressure on pyrolysis of black liquor: 2. Char yields and component release. Bioresour Technol 99:671–679. doi:10.1016/j.biortech.2006.11.064
22. Whitty K. (1997) Pyrolysis and gasification behavior of black liquor under pressurized conditions. Department of Chemical Engineering, Åbo Akademi University